Nanotribological Studies on Polymers

René M. Overney

This article seeks to review some recent studies of scanning force microscopy (SFM) and friction force microscopy (FFM) in the new field of polymeric nanotribology. The importance of surface properties, rather than bulk-material properties, in tribology is emphasized. The following aspects are discussed: indentation and scratching experiments of polymer films, failure of adhesion of pretreated polymer surfaces, stretched and strained polymers on the surface, contrasting results between surface forces apparatus and SFM/FFM, molecular lubrication, morphological and mechanical changes because of variation in the sample preparation, and wearless friction on the molecular scale. Finally, some critical comments on the adhesion concept of friction for wearless dynamic friction are added.

In the past, surface force microscopy (SFM), friction force microscopy (FFM) and the surface forces apparatus (SFA) have been very successfully applied in the study of polymer films[1–6], polymer melts[7] and diluted polymer liquids[8,9]. With SFM measurements, ultrathin self-assembled organic model systems were investigated from the aspect of boundary lubrication, where fluids behave like solids[10]. Morphology, friction and elastic compliances were simultaneously measured on the submicrometer scale[1]. Also, the viscoelastic properties of thin organic films were investigated[11]. The strength of SFM is its local sensitivity to a diverse number of material properties. Polymeric liquids were primarily studied with the SFA, which provided results concerning material properties in confined geometries. This article does not aim to review the impressive SFA work that has been published over the years; its focus is on recent SFM progress in polymeric nanotribology.

SFM is a simple but very efficient technique to study surfaces on the submicrometer scale. The principle on which it works is very similar to profilometry, where a hard tip is scanned across the surface and its vertical movements monitored. As a result of the miniature size of the SFM tip, which is mounted at the bottom end of a cantilever-like spring, it is possible to image the corrugation of the surface potential of the sample[12].

The SFM derives from the scanning tunneling microscope (STM), which was introduced by Binnig and Rohrer[13] in 1982. The STM is the first real-space imaging tool with the capability of atomic-scale resolution. But the STM is limited to imaging conducting surfaces.

René M. Overney Exxon Research and Engineering Company, 1545 Route 22 East, Annandale, NJ 08801, USA (Fax: +1-908 730 3344).

In 1986, Binnig *et al.* developed the SFM, which is capable of imaging both conductive and insulating surfaces[14]. A year later, the SFM was used to measure lateral forces that occurred during sliding contact[15].

Three more years passed after these initial and promising lateral-force results before the FFM was introduced[16,17]. The FFM is a modified SFM with a four-quadrant photodiode, based on the laser beam deflection technique[18] (see Fig. 1). The beam is emitted by a low-voltage laser diode and reflected from the rear side of the cantilever to the four-quadrant photodiode. With this detection scheme, normal and torsional forces can be measured simultaneously. The torsional forces correspond to the lateral forces measured with the instrument of Mate *et al.*[15] In 1993, Overney *et al.* introduced the threefold measurement of topography, friction and elasticity on a polymer sample using FFM[1]. With this latest achievement, a wide spectrum of tribological information was opened up, limited only by the lattice parameters of the sample.

Although SFM has been widely used in studies of polymer surfaces, only a few of these, until recently, have applied this powerful technique to tribological problems. However, more-recent work has provided new insight into the wear behavior and lubrication of polymer films on the submicrometer scale.

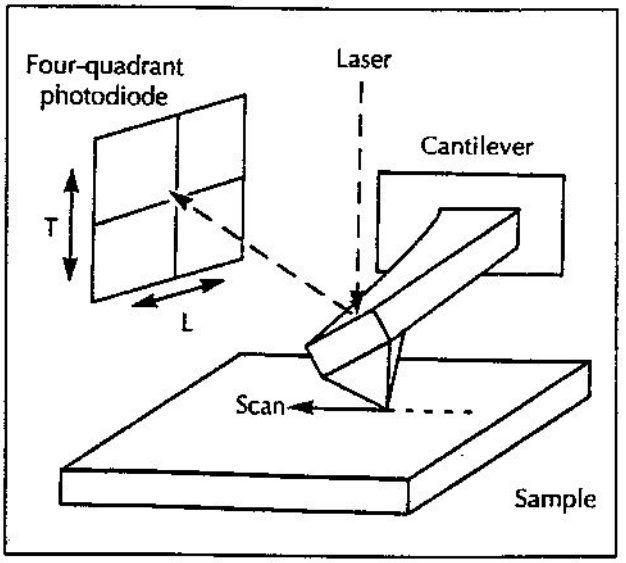

Fig. 1 *Sketch of a friction force microscope (FFM) with beam-deflection detection scheme. Cantilever movements are monitored by a laser beam with a four-quadrant photodiode. Topography (T) is measured simultaneously with lateral forces (L). Irreversible lateral forces are by definition frictional forces.*

Surface hardness

Theoretical calculations[19,20] show that the SFM tip, operating in contact mode, can cause a significant distortion of the electronic and atomic structure of the measured materials. The SFM tip is therefore well suited as a micromechanical tool. A modified SFM was used in indentation and scratch tests on polycarbonate (PC), poly(methyl methacrylate) (PMMA) and epoxy (EP) surfaces[2]. With a sharp diamond tip and a penetration load of 500×10^{-9} N, indentations 50 nm wide were created, and their profiles subsequently analyzed with the same instrument at a lower load of 50×10^{-9} N. Comparison with a conventional micro-Vickers hardness tester showed significant differences. In the Vickers hardness test, PC and PMMA showed similar indentation marks, which are about a third larger than in EP. In the SFM test, the indentation depth of PMMA is comparable to that for EP, and half that for PC. Hamada and Kaneko conclude that the discrepancies between these two tests are due to differences in the operating regime. Compared to the SFM, the Vickers hardness tester operates with a much larger volume of material, and its applied load is ten orders of magnitude higher than that of the SFM test. Therefore, the Vickers hardness test is more sensitive to bulk properties of the material, and the SFM test primarily probes the mechanical properties of the surface.

Similar results were reported by another group from scratching experiments on PC (Ref. 3). With Si_3N_4 cantilevers and applied loads of 10^{-7} N, line structures were formed with an indentation depth of 10 nm and 70 nm width. Jung *et al.* calculated from this experiment an average indentation pressure of the order of 10^7 N m^{-2} and compared it to the bulk compressive strength of PC, which is about 90 N m^{-2}. Since an indentation pressure of the order of 10^7 N m^{-2} is not expected on the macroscopic scale with an indentation depth of only 10 nm, the authors concluded that hardness at small loads must be much higher than measured with macroscopic testers.

With this observation the term 'surface hardness' was introduced for the new material property. Its technical importance is obvious for micromotors and micromachining. Future experiments and theories will show the influence of surface hardness on macroscopic quantities. The origin of the surface hardness is a fascinating problem. The key lies in a better understanding of the surface hardness on the molecular scale and its relation to the surface tension. It has been suggested that the difference between the bulk and surface hardness is maybe due to a change of the network structure at the surface and/or the capability of the surface to reconstruct faster than the bulk to adjust to external changes.

Adjustment mechanisms in scratch experiments

With contact radii of the order of a nanometer and pressures in the region of a gigapascal, single molecular rearrangements of soft organic films can occur during SFM and FFM scratch tests[4,10].

One mechanism of such molecular adjustments from high-pressure scanning is termed 'chemical' deformation of the surface in the literature[4]. The destruction of physical crosslinks in the polymer network is an example of a 'chemical' deformation[4]. 'Chemically' deformed surfaces are altered with respect to their frictional resistance[4].

'Chemical' deformations were studied by Haugstad *et al.* on AgBr–gelatin by SFM and FFM[4]. Friction measurements on scratched areas revealed heterogeneities in the polymer network[4]. The authors claim that high-force scanning of a fibrous network structure of a nominally dry gelatin gel presumably destroys physical crosslinks and initially yields another material that exhibited much higher friction forces.

Another adjustment mechanism is a 'mechanical' deformation of the surface, which is either elastic or plastic[10]. After scratch tests, the surface remains with the frictional resistance of the initial material. 'Mechanical' deformation has been studied in scratching experiments on phase-separated mixtures of fluorocarbons and hydrocarbons[10]. Low friction was observed on the easy-to-scratch hydrocarbon areas and high friction on the fluorocarbons. The fluorocarbon films were capable of withstanding normal pressures as high as 10^9 N m^{-2}. Wear could be observed on the hydrocarbon domains not only by increasing the load but also by decreasing the sliding velocity[21]. Detailed studies[21] of this effect led the authors to the idea of time-dependent bond formation[10] between cantilever and sample, which tends to minimize the surface energy. An explanation of the stability of the fluorocarbon films is perhaps found in the lower cohesive energy of these films[22] and their softer compliance response, which were revealed in the threefold measurements[1] (see below). SFM and FFM have recently been employed to explore the contact mechanics of polymer surfaces[10]. Since most techniques used in stress measurements in tribology average over macroscopically large areas or are relatively insensitive to surface phenomena, micro- or nanoindentation and scratch experiments with SFM and FFM are very promising for probing surface-related phenomena.

Surface morphology and treatments

As discussed above, the SFM can be used as a micromechanical tool. In this section, the capability to image shear forces that can be used to study surface-altering effects is highlighted. From SFM studies it is known that exposing isotactic polypropylene (PP) films to corona discharge alters the surface morphology of the film[23]. Such corona-discharge treatments are widely used for surface activation to improve the adhesion of polyolefins[24]. An excessive corona dose, however, causes deteriorative effects on uniaxial and biaxial stressed PP films, as determined from SFM investigations together with peel-experiments[23]. Figure 2a shows droplet-like structures on a striated PP film caused by an excessive corona-discharge exposure of 112.5 J cm^{-2}. The droplets appear on the surface above a critical energy dose of 18 J cm^{-2}. Their heights and diameters increase linearly with the energy dose, Fig. 2b. The appearance and the size of the droplets correspond with peel-force experiments (high peel-forces at low energy doses where there are no droplets on the surface, and decreasing peel-forces with increasing droplet size), Fig. 2b[23], which points to the droplets as the origin of the loss of adhesive strength. Further investigations were undertaken with the FFM to explore the nature and shear properties of the droplets[25]. Higher sliding friction was found on the droplets, indicating that the molecules in the droplets are more mobile than those in the bulk. This was supported by GPC

and attenuated total reflection measurements[23], which showed that the molecules of the droplets were of low molecular weight and chemically different from the untreated polymer surface. This suggests local surface melting or sublimation as a possible explanation for the formation of the droplets. With high-load scans of the order of 10^{-6} N the droplets could be moved and, with the FFM, shear forces of 2.2×10^{-5} N measured. The shear forces could be related to the surface energy[26].

Surface-altering processes under stress conditions were also investigated *in situ* with the SFM. Hild *et al.* stretched hard elastic PP films and studied the structural deformation on the nanometer scale[27]. The lamellae of strained and unstrained hard elastic PP films could be imaged, allowing the separation distance of the lamellae to be measured *in situ*. In Fig. 3, the measured interlamellar distance is plotted as a function of the elongation of the film and compared to the microscopic two-phase model proposed by Noether and Whitney[28]. In Noether's quasi-elastic model (void formation model) the strained lamellar unit length, l_s, is calculated as:

$$l_s = l_u(1 + \epsilon)$$

$$l_u = c + a$$

where l_u is the unstrained lamellar unit length, c the crystalline lamellar thickness, a the interlamellar separation and ϵ the fraction of elongation of the film. The lamellar unit is determined to be 26±3 nm (Ref. 27). For an elongation ratio smaller than 35–40%, Noether's quasi-elastic model is in good correspondence with the SFM measurements. Beyond an elongation of 40%, the measurements deviate from the model, indicating that plastic deformation occurs.

The SFM and the FFM were used in these two studies as real-space microscopic tools studying *ex situ* and *in situ* the effect of external stresses on polymer surfaces. As discussed above, an SFM study *ex situ* on corona-discharge-altered PP surfaces has been conducted along with a large variety of complementary experimental techniques. The SFM detection of droplets explained the failure in the self-adhesive properties of PP through extensive corona-discharge treatment, and directed research towards the use of GPC and attenuated total reflection. It is a good example of synergism, where the SFM/FFM plays its part as a very surface-sensitive tool by imaging morphological changes on the submicrometer scale. In an SFM study (reviewed above)[27], a theoretical strain–stress model that seems very simplistic could be tested *in situ* while the polymer film was stressed by a stretch apparatus. This experiment is an example of how easily the SFM tool can be extended, providing fundamental insight into elastic and plastic deformation of polymer films under stress.

Microscopic liquid lubrication

Polymers play an important role in the lubrication process: as viscosity modifiers (non-Newtonian behavior) to provide shear thinning; if functionalized, as wear-protective coatings and easy-to-shear boundary layers; and as anticorrosive additives by embedding (neutralizing) wear particles. Therefore, an improved fundamental understanding of polymer surfaces is desirable. Various

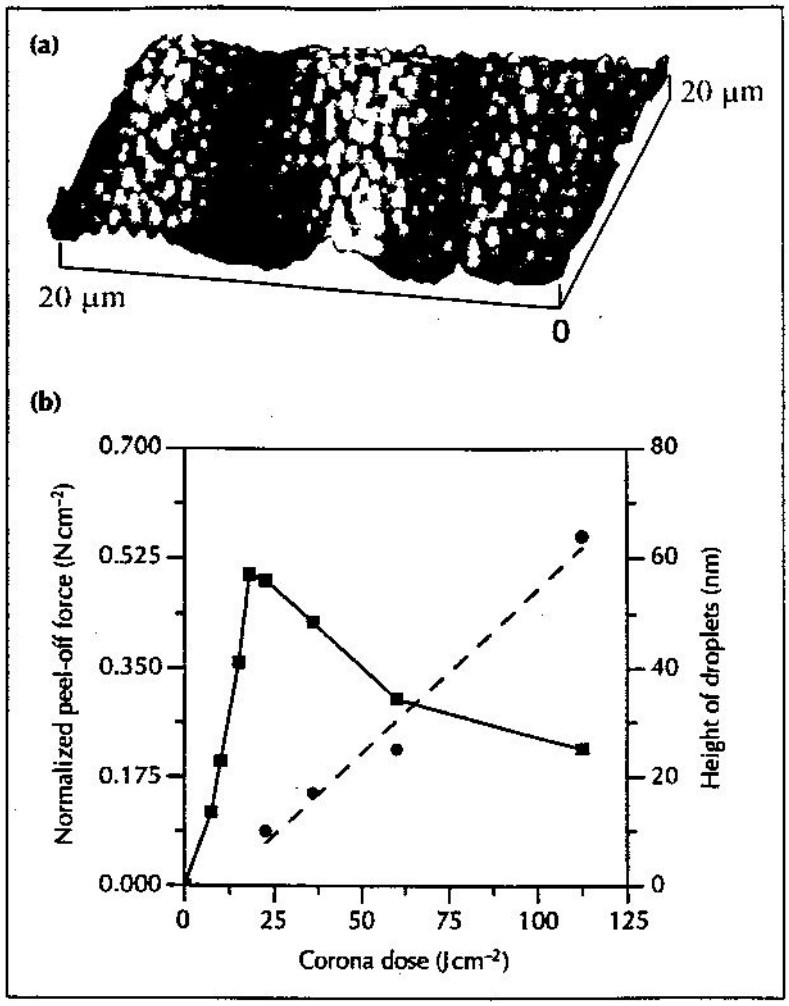

Fig. 2 *(a) A 20 × 20 µm² SFM image of a striated uniaxial PP surface. The surface was corona-discharge treated with a energy dose of 112.5 J cm⁻². The height of the droplet-like protrusions and the diameter variation of the polymer film are 64 nm and 400 nm, respectively. (b) Normalized peel-off force (■) compared to the height of the droplets (●) as functions of corona dose. At a corona dose of about 18 J cm⁻² a maximum peel-force is reached. After this critical energy dose, droplets appear on the surface, and linearly increase in size with the discharge energy.*

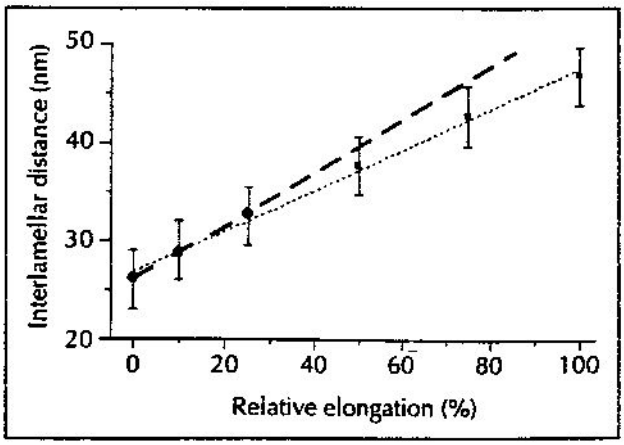

Fig. 3 *Plot of changes in interlamellar distances as a function of the strain elongation of the film (· · · ·). The plot is superimposed with Noether's quasi-elastic model [(– – –) corresponds to a linear fit of the first three data points]. Deviations from the model are noticeable above an elongation of 40% (plastic deformation). (Modified from Ref. 27.)*

adopted and followed up Desanguliers' hypothesis[38] that claims adhesion as an element in the friction process. The second Amontons' law states that friction is independent of the contact area. However, adhesive forces are well known to depend on the contact area. Therefore, the adhesive concept of friction initially caused a contradiction. This contradiction was cleared up by the introduction of the concept of the 'real area' of contact. The real area of contact integrates over a large number of small regions of contact, called asperities. Bowden and Tabor defined the adhesive part of friction as the product of shear strength and the real area of contact[34]. The adhesive part of friction has been shown to play a dominant role in metal–metal contact[38]. Yet their results are not necessarily valid for other materials. Also, there are problems in extending their results to dynamic friction. In particular for thin polymeric films, mechanical properties are expected to dominate adhesive properties in wearless dynamic dry friction measurement, as reviewed above. The surface potential and the viscoelastic behavior have been found to be responsible for dry friction of polymeric systems[1,4,10,12]. The work that has been done up to now with a simplified, geometric, experimental setup, the single asperity FFM contact, is very promising, and I expect that in the next few years a major breakthrough in nanotribology, as was achieved by the adhesive concept in classical tribology, will be achieved.

Little work has been done, so far, by FFM on polymer melts and liquids. Most of our insight into material properties of confined liquid polymers has been provided by SFA[7–9]. Mate showed that SFA and FFM studies performed in parallel can produce an enhanced understanding of the behavior of liquid polymers under stress[9]. One major difference between the two techniques is in the contact area (about three orders of magnitude, i.e. square micrometers and square nanometers for SFA and SFM, respectively). Both systems are very sensitive and capable of measuring forces on the tenths of nanometers scale. Depending on the characteristics of the liquid polymer system (e.g. the molecular mobility), SFM and FFM results can correspond or deviate from each other. Polymers that interact with the substrate are, based on a recent study (R.M. Overney *et al.*, unpublished, presented at the ACS Spring Meeting 1995 in Anaheim), good candidates for SFM compliance studies. In this study of polymer brushes dissolved in a good solvent, the results have been found to correspond well with SFA measurements. In particular, surface active additives in lubricating liquids are expected to be very suitable for SFM/FFM experiments because they can easily be studied on any solid substrate (in contrast to SFA, which is restricted by the choice of the substrate). The critical point of the FFM technique is the estimation of the contact area. A quantitative analysis is crucial. Therefore, combined SFM/FFM and SFA studies are recommended.

Our understanding of polymer surfaces is much improved by performing experiments on the nanometer scale. Computer simulations and models can easily be confirmed by experiments on such small scales[12,20,27,28]. In the future, new concepts, which find their analogues in statistical mechanics and thermodynamics, may be developed because of the small contact area. One of the important future goals of the SFM and FFM techniques is to connect phenomenological aspects in tribology with

Table 1. Effect of pH on the properties of films composed of 1 : 1 molar mixtures of BA and PFECA complexed with polyallylamine (see text)[a]

Film properties	pH 4.5	pH 6.6	pH 9.3
Diameter (nm) of hydrocarbon islands	300–1000	80	100–200
Friction (hydrocarbon) (nN)	8.9	4.9	4.5
Friction (fluorocarbon) (nN)	23.5	13.4	12.6
Ratio of friction (hydrocarbon : fluorocarbon)	1 : 2.5	1 : 3	1 : 3
Elastic compliance (GPa) on hydrocarbon islands	0.4	0.2	0.2

[a]Data from Ref. 1.

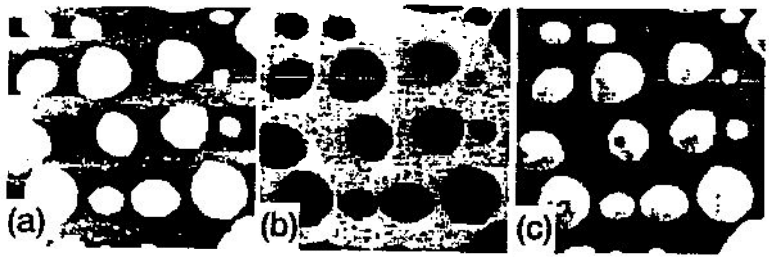

Fig. 4 *Threefold measurement (3×3 μm²) of topography, friction and elasticity with SFM. (a) Topography with island-like hydrocarbon domains (bright) of about 300–1000 nm in diameter on top of a sea-like fluorocarbon film (dark). The height of the islands is 2.5±0.5 nm. The sample was prepared at a pH of 4.5 from a 1 : 1 molar mixture of BA and PFECA. (b) Friction force map shows lower friction (dark), by a factor of 2.5, on hydrocarbon islands. (c) Elastic compliance (elasticity) map shows higher Young's modulus (bright) for the hydrocarbon domains. The relative difference in elasticity is 0.1±0.03 GPa. Elasticity measurements reveal a Young's modulus for these hydrocarbon domains that is twice as high as for those in films prepared at pH 6.6 and 9.3.*

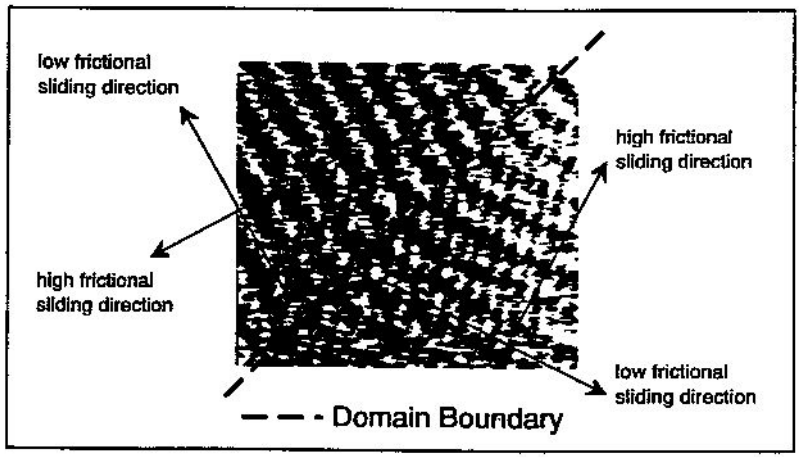

Fig. 5 *A 12 × 12 nm² FFM image of a lipid bilayer structure [5-(4'-N,N-dihexadecylamino)benzylidene barbituric acid]. Imaged is a boundary between two domains. Two alignments of rows can be observed with equivalent unit cells (1.1 nm; 0.6 nm; 72°). Sliding friction values vary depending on the scan direction and the orientation of the rows. Highest friction is observed when the rows are perpendicularly oriented to the sliding direction.*

a molecular understanding. To achieve such a goal demands from the scientists in nanotribology that they follow atomistic and statistical principles, avoid empirical formulas (or laws), such as frictional coefficients, etc., that were developed in/for macroscopic experiments, and search for conformity between experimental data and atomistic theoretical models and computer simulations.

Acknowledgements
I wish to thank M. Rafailovich, S. Kelty, S. Hild and G. Haugstad for helpful comments and discussions. The work was partially supported by the Swiss National Science Foundation and the Kommission zur Förderung der wissenschaftlichen Forschung (Switzerland).

References

1 Overney, R.M. *et al.* (1994) *Langmuir* 10, 1281
2 Hamada, E. and Kaneko, R. (1992) *Ultramicroscopy* 42–44, 184
3 Jung, T.A. *et al.* (1992) *Ultramicroscopy* 42–44, 1446
4 Haugstad, G., Gladfelter, W.L., Weberg, E.B., Weberg, R.T. and Weatherill, T.D. (1994) *Langmuir* 10, 4295
5 Monfort, J.P. and Hadziioannou, G. (1988) *J. Chem. Phys.* 88, 7187
6 Yoshizawa, H., Chen, Y-L. and Israelachvili, J. (1993) *J. Phys. Chem.* 97, 4128
7 Israelachvili, J.N., Kott, S.J. and Fetters, L.J. (1989) *J. Polym. Sci., Part B, Polym. Phys.* 27, 489
8 Taunton, H.J., Toprakcioglu, C., Fetters, L.J. and Klein, J. (1990) *Macromolecules* 23, 571
9 Mate, C.M. (1991) *Phys. Rev. Lett.* 68, 3323
10 Overney, R. and Meyer, E. (1993) *MRS Bull.* 18, 26
11 Radmacher, M., Tillmann, R.W., Fritz, M. and Gaub, H.E. (1992) *Science* 257, 1900
12 Overney, R.M., Takano, H., Fujihira, M., Paulus, W. and Ringsdorf, H. (1994) *Phys. Rev. Lett.* 72, 3546
13 Binnig, G. and Rohrer, H. (1982) *Helv. Phys. Acta* 55, 726
14 Binnig, G., Quate, C.F. and Gerber, C. (1986) *Phys. Rev. Lett.* 56, 930
15 Mate, C.M., McClelland, G.M., Erlandsson, R. and Chiang, S. (1987) *Phys. Rev. Lett.* 59, 1942
16 Meyer, G. and Amer, N.M. (1990) *Appl. Phys. Lett.* 57, 2089
17 Marti, O., Colchero, J. and Mlynek, J. (1990) *Nanotechnology* 1, 141
18 Meyer, G. and Amer, N.M. (1988) *Bull. Am. Phys. Soc.* 33, 319
19 Abraham, F.F. and Batra, I.P. (1989) *Surf. Sci.* 209, L125
20 Overney, G. (1993) in *Scanning Tunneling Microscopy III* (Wiesendanger, R. and Güntherodt, H-J., eds), pp. 251–268, Springer-Verlag
21 Overney, R.M., Takano, H., Fujihira, M., Meyer, E. and Güntherodt, H-J. (1994) *Thin Solid Films* 240, 105
22 Hildebrand, J. and Scott, R. (1965) *The Solubility of Nonelectrolytes* (3rd edn), pp. 436–438, Dover Publications
23 Overney, R.M. *et al.* (1993) *Appl. Surf. Sci.* 64, 197
24 Kim, C.Y., Suranyi, G. and Goring, D.A.I. (1970) *J. Polym. Sci., C, Polym. Lett.* 30, 553
25 Overney, R.M., Güntherodt, H-J. and Hild, S. (1994) *J. Appl. Phys.* 75, 1401
26 Laveielle, L. (1989) *Ann. Phys.* 14, 1 [French edn]
27 Hild, S., Gutmannsbauer, W., Lüthi, R., Fuhrmann, J. and Güntherodt, H-J. *J. Polym. Sci.* (in press)
28 Noether, H.D. and Whitney, W. (1973) *Kolloid-Z. Z. Polym.* 251, 991
29 Gisser, D.J., Johnson, B.S., Ediger, M.D. and von Meerwall, E.D. (1993) *Macromolecules* 26, 512
30 Gee, M.L., McGuiggan, P.M., Israelachvili, J.N. and Homola, A.M. (1990) *J. Chem. Phys.* 93, 1895
31 Granick, S. (1992) in *Fundamentals of Friction: Macroscopic and Microscopic Processes* (Singer, I.L. and Pollock, H.M., eds), pp. 387–401, Kluwer
32 Floudas, G. (1994) *J. Non-Cryst. Solids* 172–174, 729
33 Mate, C.M. and Novotny, V.J. (1991) *J. Chem. Phys.* 94, 8420
34 Bowden, F.P. and Tabor, D. (1954) *Friction and Lubrication of Solids* (Part 1), Clarendon Press
35 Subramanian, G., Williams, D.R.M. and Pincus, P.A. (1995) *Europhys. Lett.* 29, 285
36 Meyer, E. *et al.* (1992) *Thin Solid Films* 220, 132
37 Nishiyama, K., Kuishara, M. and Fujihira, M. (1989) *Thin Solid Films* 179, 477
38 Dowson, D. (1979) *History of Tribology*, Longman

Forthcoming Trends

The topics that will be covered in forthcoming issues of *Trends in Polymer Science* include:

- Recent developments in the treatment of cotton
- Cationic polymerization: past – present – future
- The topological modification of DNA and RNA
- New gelling agents from bacterial alginates
- Light-harvesting polymer catalysts
- Nanorheology of polymers
- The use of microwaves in the processing of polymer composites
- Fullerenols and conducting elastomeric films
- Mass spectrometry of synthetic polymers
- Degradable polyamides and related polymers
- Glass transition temperatures from molecular dynamics simulations
- Hydrogels based upon fluorosiloxanes